Available online at www.sciencedirect.com
ScienceDirect
Cement & Concrete Composites 29 (2007) 70–79
Cement & Concrete Composites
www.elsevier.com/locate/cemconcomp

Correlation of fiber dispersion, rheology and mechanical performance of FRCs

Nilufer Ozyurt [a,*], Thomas O. Mason [b], Surendra P. Shah [c]

[a] Faculty of Civil Engineering, Istanbul Technical University, Istanbul 34469, Turkey
[b] Department of Materials Science and Engineering, Northwestern University, 2145 Sheridan Road, Evanston, IL 60208, USA
[c] Center for Advanced Cement Based Materials, Northwestern University, 2145 Sheridan Road, Evanston, IL 60208, USA

Received 23 January 2006; received in revised form 21 August 2006; accepted 31 August 2006
Available online 19 October 2006

Abstract

Fresh state properties of fiber-reinforced concretes (FRCs) were correlated to hardened state properties by quantifying fiber segregation. Rheological characteristics were evaluated using a custom-designed and built parallel-plate rheometer. Fresh state properties of concrete mixes were varied using different combinations of plasticizing agents and viscosity modifiers. Vibration was applied to the specimens and vibration times were varied to understand the effects of vibration on fiber segregation. Two sizes of steel fibers were used. Alternating current-impedance spectroscopy (AC-IS) was employed to non-destructively characterize fiber segregation in the specimens. In addition, fiber segregation was experimentally quantified using a destructive technique in which the amount of fibers in different regions is weighed. A self-compacting concrete (SCC) mix was cast to compare segregation resistance with conventional concretes (CC). Splitting tensile tests were performed to study mechanical performance of FRC specimens. The effects of the rheological characteristics on fiber segregation and, consequently, on the mechanical performance is discussed.

Keywords: Fiber dispersion; Rheology; AC-impedance spectroscopy; Self-compacting concrete; Fresh state properties

1. Introduction

Characteristics of fiber dispersion affect fresh state properties of FRCs and vice versa. Considering that mechanical performance is strongly related to (i) fresh state properties and (ii) fiber dispersion characteristics, it is essential to control both parameters for a superior mechanical performance.

The importance of rheological characteristics on the mechanical performance of cement-based materials has long been known and extensive research has been done on the subject. Various equipment and methods are used to measure and define rheological properties. Unfortunately, standardized equipment and measuring methods are not yet established [1]. One reason for this lack of standardization is that the rheology of cement-based materials is dependent on many parameters [2]. It is hard to use one single equipment to define characteristics of materials with different properties and constituents (cement, mortar, concrete, fiber-reinforced cement-based materials, etc.) [3]. Depending on the material type, one has varying aspects to consider, such as the effect of aggregate size when studying concrete, or effect of fiber orientation when studying the rheology of fiber-reinforced materials. In this study, a custom-designed and built parallel-plate rheometer is used for studying fresh state properties of cement paste. The rheometer was specifically designed to study fresh state properties of stiff cementitious materials. Details related to the design and verification of the parallel-plate rheometer were discussed in a previous paper [4]. The use of this rheometer made possible the measurement of the rheological characteristics of stiff cementitious materials, including fiber-reinforced and highly viscous mixes.

* Corresponding author. Tel.: +90 2122856792; fax: +90 2122856587.
E-mail address: ozyurtnil@itu.edu.tr (N. Ozyurt).

0958-9465/$ - see front matter © 2006 Elsevier Ltd. All rights reserved.
doi:10.1016/j.cemconcomp.2006.08.006

Fibers have long been used in cement-based materials to obtain enhanced material performance. Substantial increase in tensile strength and toughness is the most acknowledged feature of fiber-reinforced composites [5,6]. Some of the other benefits gained using fibers are increased shear strength [7], increased resistance to dynamic loads [8] and reduced shrinkage cracking [9]. In the last decades new materials such as engineered fibers [10] and engineered cementitious composites (ECC) [11,12] have been developed to effectively use fibers and obtain features such as superior mechanical performance and durability. The reinforcing ability of fibers depends on how the fibers are dispersed throughout the material [13,14]. Poorly dispersed fibers provide little or no reinforcement in some regions, which then act as flaws in the composite material. Uniformly dispersed fibers minimize the largest size of such flaws and, therefore, maximize the reinforcement efficiency. Problems related to fiber dispersion are likely to be encountered when using FRC materials and controlling fiber dispersion characteristics is generally difficult. New methods are needed to control fiber dispersion characteristics. However, for this to be done, convenient methods are needed for evaluating fiber dispersion since most methods currently used are both destructive as well as time consuming. Recently, an electrical characterization method – alternating current-impedance spectroscopy (AC-IS) – was proposed to define fiber dispersion characteristics of FRC materials. AC-IS was found to be effective for monitoring various fiber dispersion issues such as fiber orientation, segregation and clumping [15,16]. Characteristics of fiber dispersion were evaluated using an intrinsic conductivity approach. AC-IS was compared with more conventional methods (time and labor intensive image analyses). Model studies on lab-size specimens were extended to industrial-scale specimens and promising results were obtained [16–18].

In this study, AC-IS was used to monitor fiber segregation in steel fiber-reinforced cement-based specimens. The main objective of this study is to connect fresh state properties to the hardened state properties by quantifying fiber dispersion. If both rheological properties and fiber dispersion can be controlled, and the effects of both parameters on the mechanical performance are well-known, quality control and quality assurance can be provided.

2. Fundamentals of the methods

2.1. AC-IS

Impedance spectroscopy is a popular analyzing tool that is widely used in various fields of research such as physical chemistry, electrochemistry, physics, materials science, etc. The use of IS to study various features of cement-based materials goes back to late 1980s. From this date, the use of IS to study cement-based materials has increased and IS has been used for studying various phenomena in cement-based materials, including hydration development [19], transition properties (permeability, diffusivity) [20], structural health monitoring [21] or damage monitoring [21–23]. Research regarding the use of IS to investigate particle-reinforced composite systems led to an understanding of a unique frequency-dependent behavior [24,25]. Conductive fibers were shown to be insulating under low frequencies of AC while they are conductive under high frequencies. This phenomenon occurs due to either an oxide film (e.g., on steel fibers) or a polarization layer (i.e., double layer/charge transfer resistance) forming at the fiber-electrolyte interface. Fig. 1 shows Nyquist curves of plain cement paste and steel fiber-reinforced cement paste. As seen in the figure, cement paste shows only one bulk arc to the left of the electrode arc (rightmost arc), while FRC specimen shows two bulk arcs. In the impedance curve of FRC specimens, the rightmost cusp gives matrix resistance, R_m (low AC frequencies – fibers act insulating), and the leftmost cusp gives the resistance of the fiber + matrix composite system, R_c (fibers are conductive). The solid data points on the curves are given for the frequency at these points and shown as $\log_{10} f$ (for example, for 100 Hz, $\log_{10} 100 = 2$). Direct current (DC) measurements are sometimes done to verify the low-frequency results of AC-IS, as shown in Fig. 1.

To obtain AC-IS measurements, a voltage excitation over a range of frequencies is applied to specimens and the magnitude and phase of the current is measured. The real and imaginary parts of impedance are then calculated and plotted on a Nyquist diagram. Matrix-normalized conductivity (σ/σ_m) is used to define fiber dispersion characteristics from experimental data, where σ is the conductivity of the composite when the fibers are conducting (comes from R_c) and σ_m is the conductivity of the matrix (comes from R_m).

Previous work of the authors has shown that by making use of the dual-arc behavior, it is possible to monitor various fiber dispersion issues in FRC specimens. A comprehensive experimental work was carried out to understand the ability of AC-IS for monitoring fiber dispersion characteristics. Experimental findings were mathematically

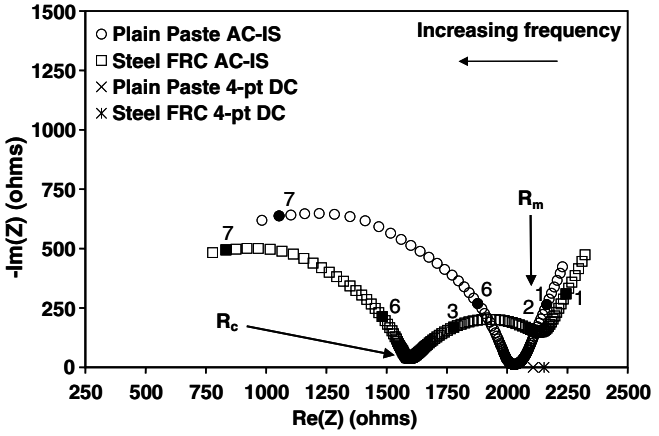

Fig. 1. Typical Nyquist curves for plain paste and fiber-reinforced cement paste.

expressed using an intrinsic conductivity approach to define the level of dispersion. AC-IS was compared with a fundamental method to understand the extent to which AC-IS predicts features of fiber dispersion. Results showed great promise [16–18]. Then, an industrial-scale application of the method was done on a structural FRC beam to evaluate the applicability of AC-IS on larger-scale specimens. The details and results of the previous experimental work can be found in [15–18,26]. In this study, AC-IS is used to non-destructively monitor fiber segregation in cylindrical FRC specimens.

2.2. Rheology

A custom-designed and built parallel-plate rheometer was used to obtain yield stress and viscosity of cement paste and mortar (Fig. 2). Yield stress can be defined as the force required to initiate flow and viscosity is the resistance to flow. Detailed information regarding the design and verification of the rheometer is discussed in another paper [4]. A short review of the properties of the equipment and measuring protocol is given here. The rheometer includes two parallel-disks and a plexi-glass wall. The parallel-plates used were 254 mm in diameter and their surfaces were roughened using square grooves (measuring $6.3 \times 6.3 \times 2.5$ mm) to minimize slip. A plexi-glass wall was attached to the bottom plate to prevent material from flowing away. The gap height is adjustable and can go up to 25 mm. A high torque capacity motor (20 N m) is used for testing high viscosity materials (with low water-to-cement ratios). The upper plate rotates at a controlled speed and the bottom plate is stationary. The shear rate (the rate of change of shear strain with time) varies along the radius of the disks as seen in Fig. 2(c).

The frictional effect of the wall was accounted for in the calculations and experiments were conducted to better understand the effect of wall. Results of the experiments showed that the effect of the wall on the yield stress was minimal and could, therefore, be neglected. Viscosity was found to change with varying gap heights. However, it was possible to define an optimal range for the gap height in which the wall effect and teeth effect could be minimized. For the sake of time and simplicity, the gap height was kept constant at this range (10–13 mm) for all of the experiments.

2.3. Rheology measuring protocol

A measuring protocol that was similar to the one used by Geiker et al. [27] was applied. The material was sheared for 20 s to ensure an equilibrium condition at each shear rate. Torque measurements were obtained for 20 s, as seen in Fig. 3, and values corresponding to equilibrium region

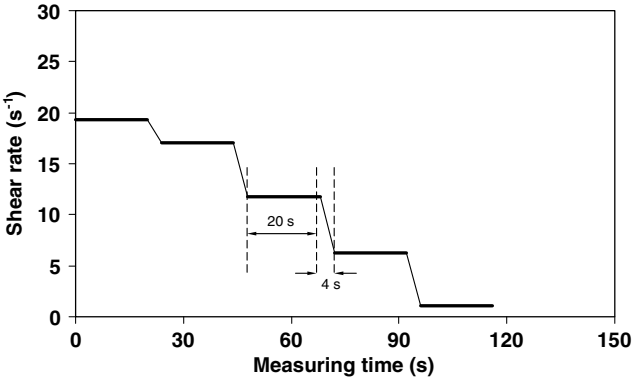

Fig. 3. Measuring protocol.

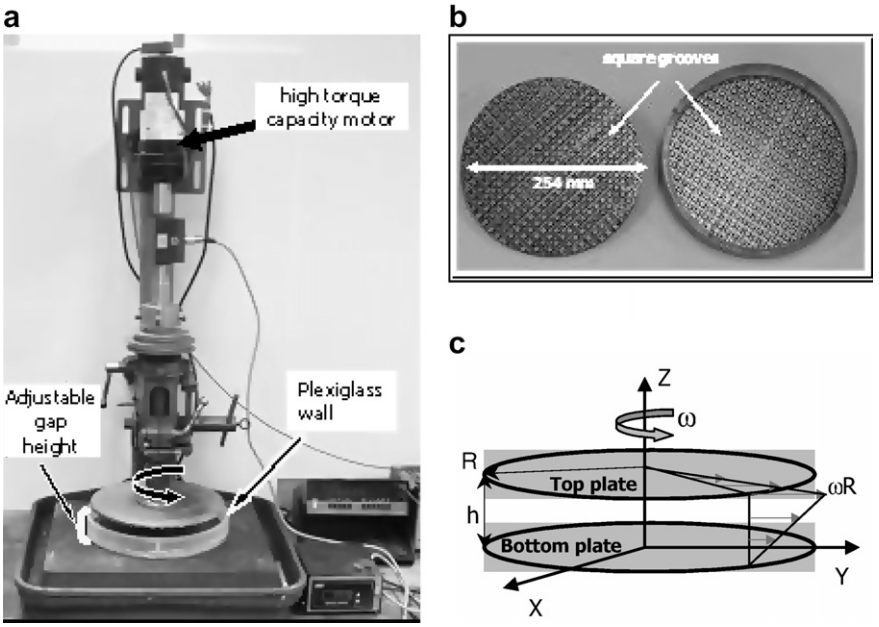

Fig. 2. (a) Custom-designed parallel-plate rheometer, (b) plates, and (c) distribution of shear rate.

were averaged to obtain torque at each shear rate. Shear stress and shear rate were calculated using the torque and rotation speed. The Bingham model was employed to obtain rheological characteristics from shear stress and shear rate. Yield stress was obtained using the lowest two data points (the shear stress values that correspond to lowest shear rates) and extrapolating to the y-axis, since the yield stress corresponds to the shear stress at a gap height of zero. Viscosity (differential) was calculated as the gradient of the shear stress vs. shear rate curves.

3. Experimental work

3.1. Materials and mix designs

Fiber-reinforced concrete specimens were cast and various vibration times were applied. LaFarge Type I Portland cement and two types of steel fibers were used. Short-cut straight steel fibers with 6 mm long and 0.16 mm diameter (OL 6/0.16) and longer steel fibers with 40 mm long and 0.62 mm diameter (Dramix RC-65/40 hooked end fibers) were provided by Bekaert and used in different mixes. Daracem 19 by W.R. Grace was the superplasticizer (sp) used in all mixes except for the SCC mix. For SCC, a polycarboxylate-based superplasticizer produced by Axim Italcementi Group was used. The viscosity modifying agent (vma) was Kelcocrete 1376 by CP Kelco. The river sand had a maximum diameter of 3 mm and the coarse aggregate had a maximum diameter of 8 mm. The water-to-cement ratio was kept constant at 0.40. The fiber loading was 1% of the total volume for all mixes. Mixing sequence and time were similar for all the mixes. The concrete mix designs and vibration times are given in Table 1 (vibrating table vibrates at 3600 VPM on 60 H power). Seven groups of concretes were cast. Each mix design is referred with letters (A, B or C) and the vibration time is given as subscript. For example, A_2 represents the design with superplasticizer and subscript 2 shows vibration time in minutes. Tables 2 and 3 show mix designs for conventional concrete mixes and SCC, respectively.

Three cylinders with dimensions of 15×30 cm (6 in. $\times$ 12 in.) were cast for each group. One specimen of each group was used for the fiber content calculation in the fresh state and two specimens were left for curing under 100% relative humidity. Non-destructive AC-IS measurements were carried out on one of these specimens after 3 days and splitting tensile test was done on the third specimen at 14th day.

Table 1
Concrete mix designs and vibration times

Fiber type	Mix design		Vibration time
6 mm fibers $w/c = 0.40$ Fiber content: 1% vol.	A_0	sp	No vibration
	A_2		2 min
	A_8		8 min
	B_8	sp + vma	8 min
	C_8	vma	8 min
40 mm fibers $w/c = 0.40$ Fiber content: 1% vol.	A_2	sp	2 min
	SCC	sp	No vibration

Table 2
Conventional concrete mix design

Cement	Water	Fine agg.	Coarse agg.	Vma (% water weight)	sp (% cement weight)	Fiber (% vol.)
1	0.4	2	2	0.2	1	1

Table 3
SCC mix design

Cement	Water	Fine agg.	Coarse agg.	Fly ash	sp (% bind. weight)	Fiber (% vol.)
1	0.4	1.56	1.9	0.25	0.7	1

3.2. Measurement of fiber content in the fresh state

One specimen of each group was cut into 4 pieces immediately after initial set, fibers were washed out and fiber volume ratios in each part were calculated. Measured fiber contents were than used for calculating theoretical matrix-normalized conductivity values. Fig. 4 shows a schematic of the slicing of the specimens. The slices were notated from a to d beginning from the top of the specimen. These experiments were performed so that the AC-IS measurements could be compared with an alternate method.

3.3. Study of segregation using AC-IS

AC-IS measurements were done along the height of the cylinders. Measurements were obtained from 4 different positions from a to d. Wet sponges were used under stainless steel electrodes to ensure a good contact between the specimen and the electrodes. 1 M NaCl solution was used to wet the sponges. AC-IS measurements were done using a Solartron 1260 impedance/gain-phase analyzer, and the frequency was stepped from 100 mHz to 11 MHz under a voltage excitation of 1 V. Fig. 4 shows electrode positions

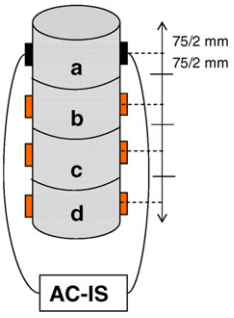

Fig. 4. Sectioning of cylinder specimens and electrode positions for AC-IS measurements.

from the top to the bottom of a cylinder specimen. Four sections were drawn on the specimens and measurements were obtained from the middle of each section as seen in Fig. 4.

3.4. Mechanical tests – splitting tensile tests

Splitting tensile tests were conducted according to a modified version of EN-12390-6. A closed-loop MTS testing machine was used with a 500 kN capacity load cell. Loading was applied under average lateral displacement control, which was monitored using 2 LVDTs (linear variable displacement transducer) that had a maximum range of 2.5 mm. The LVDTs were fixed onto each side of the specimen and the lateral displacement was monitored. Initially, loading was applied at a rate of 0.00025 mm/s. After the maximum stress was reached, the rate was increased to 0.001 mm/s (for the sake of time). Testing continued until a 2 mm lateral displacement was reached. Load and LVDT displacements were recorded for data analysis.

Fig. 5 shows the splitting tensile test. Tensile strength of each part was calculated using the equation below

$$f_{ct} = \frac{2P}{LD} \quad (1)$$

where f_{ct} is stress (MPa), P is the maximum load (N), L is the length of the line of contact of the specimen (mm), D is the cross-sectional dimension (mm) of the specimen.

3.5. Rheology

Experiments were conducted on the cement pastes of the mix designs to obtain rheological characteristics, thereby allowing for the connection of the fresh and hardened state properties of the FRCs by quantifying fiber dispersion. First, cement was placed in a Hobart mixer, and then water added to the mix (sp and/or vma added to the water beforehand, if applicable). After the cement and water were mixed for 1 min at the low speed, there was a 30 s rest. Finally, the materials were mixed for 2 min at the high speed. The rheological measuring protocol given in Fig. 3 was used. The gap height between the plates was kept between 10 and 13 mm, as mentioned in 2.2. Three repetitions were made for each mixes. Shear stress and shear rate values were calculated from torque to rotation rate measurements. The cement pastes showed Bingham behavior. Yield stress and viscosity values were calculated using Bingham plots.

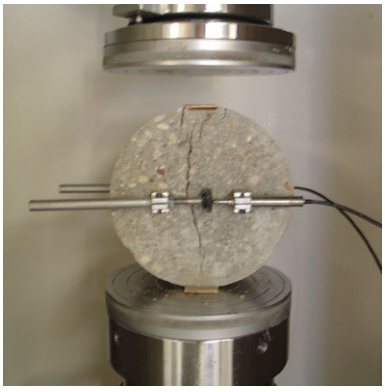

Fig. 5. Splitting tensile test set up.

4. Results and discussion

4.1. Fiber content distributions (immediately after initial set)

Fiber content distributions were obtained for each concrete mixes and are given in Table 4 and Fig. 6. The segregation of the fibers increased with increasing vibration (A_0, A_2, A_8). Mix designs with vma appeared to be more resistant to segregation even when vibration was applied. Design A_2 with 6 mm long fibers had less segregation when compared to design A_2 with 40 mm long fibers. The SCC mix had some segregation, but not as severe as the mix design A_8. These findings should also be evaluated from the density/mechanical performance point of view, which is done in Section 4.5.

4.2. AC-IS

AC-IS measurements were obtained and matrix-normalized conductivities (σ/σ_m or R_m/R_c) were calculated for each section of the specimens. Table 5 shows fiber content

Table 4
Fiber content distribution in specimens for different mix designs and vibration times

	6 mm fibers					40 mm fibers	
	A_0	A_2	A_8	B_8	C_8	A_2	SCC
a	0.99	0.90	0.38	0.89	0.97	0.70	0.92
b	0.99	0.92	1.02	0.88	1.00	0.97	1.19
c	0.96	1.02	1.20	0.97	1.00	0.98	1.08
d	0.89	1.15	1.44	0.98	1.01	1.30	1.13

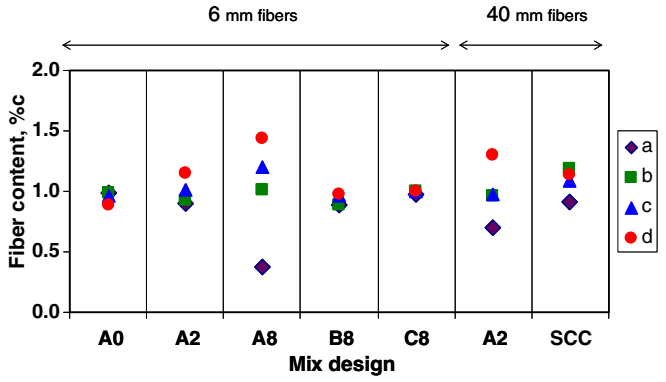

Fig. 6. Fiber content distribution in specimens for different mix designs and vibration times.

Table 5
Corrected matrix normalized conductivity values together with the observed and calculated values for mix design A_8

	Fiber content % vol.	σ/σ_m (observed)	σ/σ_m (theoretical) (calculated using Eq. (2))	σ/σ_m (corrected)
a	0.38	1.51	1.45	0.38
b	1.02	2.45	2.20	1.05
c	1.20	3.65	2.42	1.74
d	1.44	4.91	2.70	2.50

distribution in a specimen (mix design A_8), together with observed and theoretical matrix-normalized conductivities (theoretical values were calculated using measured fiber contents (φ) and Eq. (2)), where σ/σ_m stand for matrix-normalized conductivity, $[\sigma]_\infty$ represents intrinsic conductivity of fibers and φ stands for fiber content

$$\frac{\sigma}{\sigma_m} = 1 + [\sigma]_\infty \varphi \quad (2)$$

When the values in Table 5 are compared, it is seen that the observed values are excessively high compare to the theoretical values. This result can be explained by the insulating property of the coarse aggregates. The maximum diameter of the coarse aggregates is 8 mm, while the fiber length is 6 mm, meaning that the coarse aggregates are big enough to block the conductive fibers and can, therefore, cause a reduction of the concrete matrix conductivity. Mathematical expressions were used to exclude this insulating effect of the aggregates and to calculate the corrected matrix-normalized conductivities. The effect of aggregate size and the applied correction of the results are explained in the Appendix A. Table 5 shows fiber content distribution, and the observed, theoretical and corrected matrix-normalized conductivities for the design A_8. As seen in Table 5, the matrix-normalized conductivity increases with increasing fiber content. Fiber content distribution and the matrix-normalized conductivity relationship in the specimens are discussed in Section 4.4.

4.3. Mechanical tests

Splitting tensile tests were done on parts of the specimens, as was defined in 3.4. Load vs. lateral displacement curves were obtained and splitting tensile strengths were calculated. Fig. 7 shows the load–deflection curves for the specimen sections cast using mix design A_8. As is seen in Fig. 7, parameters such as tensile strength and the area under the load–displacement curve (a measure of fracture energy) are found to be higher for the bottom parts of the specimens.

4.4. Rheology

Table 6 shows viscosity and yield stress values with standard deviations for all the mixes. As seen in Table 6, the viscosity and yield stress increase with the addition of

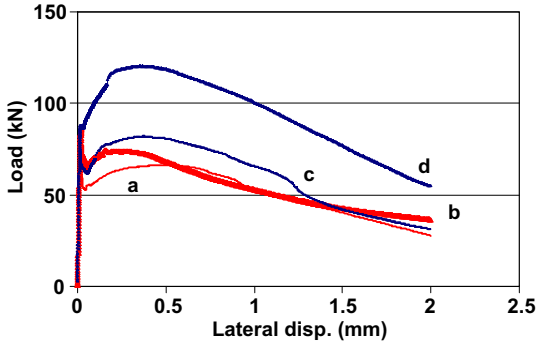

Fig. 7. Load vs. lateral displacement curves for the specimen made with the design A_8.

Table 6
Rheological characteristics of cement pastes

		Mix Design	Viscosity (Pa s)	Standard deviation (Pa s)	Yield stress (Pa)	Standard deviation (Pa)
Paste	sp	A	1.20	0.15	46.73	5.05
	sp + vma	B	3.52	0.18	110.65	2.31
	vma	C	5.45	0.29	76.73	2.07
	scc	SCC	7.22	0.51	19.48	2.80

vma and the SCC mix has the lowest yield stress and highest viscosity. The yield stress of design C was found to be lower than design B, while the viscosity is higher. This trend occurs due to the segregation preventing property of the vma used in this study. Kelcocrete 1376 is a viscosity modifier that is specifically designed to lower the segregation of the ingredients in concrete by lowering yield stress while increasing viscosity.

4.5. Comparing test results

Data from the fiber content calculation, AC-IS measurements and splitting tensile tests were plotted together for comparing the results of the experiments. Fig. 8(a)–(c) shows profiles for mix designs A_8, A_2, and SCC, respectively. As seen in Fig. 8, tendencies for fiber content and matrix-normalized conductivity distribution of specimens are very similar, suggesting that AC-IS can be used to measure fiber content or fiber segregation in FRC specimens. The distribution of the normalized-conductivity and the splitting tensile strength is also very similar, implying that the segregation of fibers negatively effect mechanical performance. Fig. 8(c) also shows that SCC is more resistant to fiber segregation than CC (b).

4.6. Correlation of fiber dispersion, rheology and mechanical performance

In this study, the performance of concrete mix designs are described by more than one parameters, including fiber segregation resistance, placeability, and mechanical perfor-

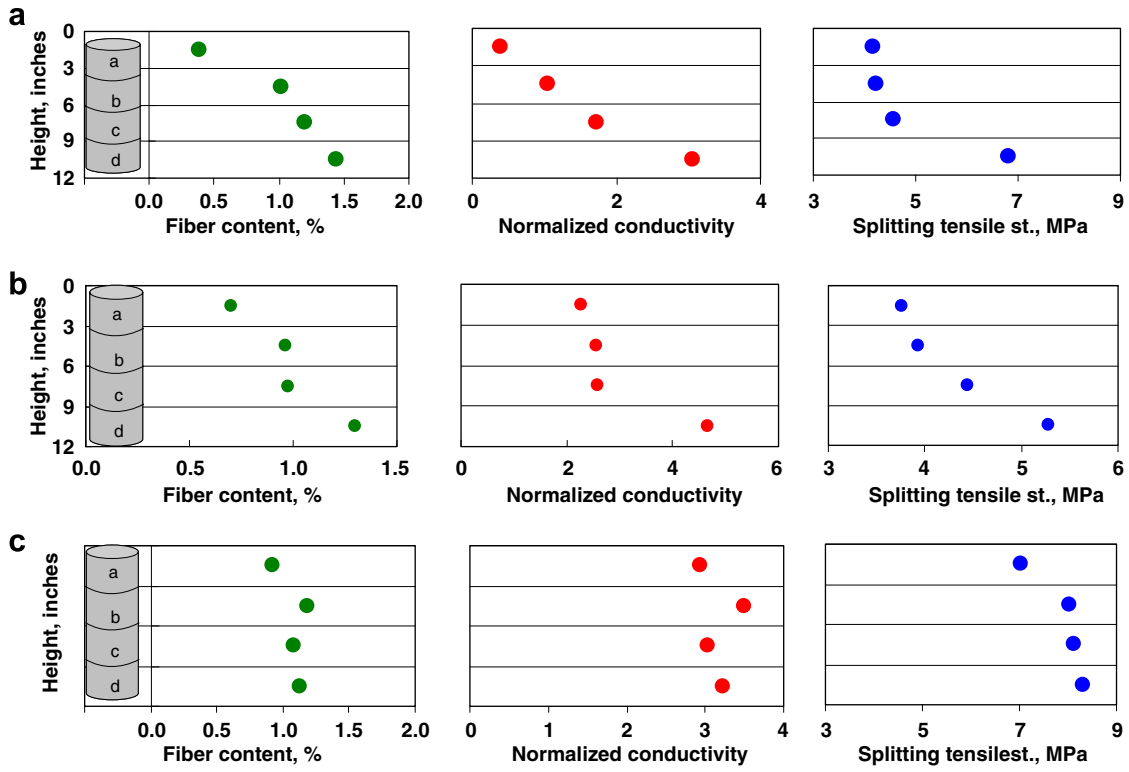

Fig. 8. Fiber content, matrix-normalized conductivity and splitting tensile strength profiles of (a) mix design A_8 (conventional concrete with sp and 6 mm fibers), (b) A_2 (with 40 mm steel fibers) and (c) SCC (40 mm steel fibers).

mance. All of these parameters are strongly related to each other and a mutual effect exists. Table 4 and Fig. 6 show that the segregation resistance of the designs with vma is higher than the segregation resistance of the designs with sp. However, this does not mean that the designs with vma are superior to designs with sp. Other properties of concrete are also significant and should be addressed as well. In this part of the study, fiber segregation resistance is evaluated together with density (a measure of mechanical performance) and placeability and remarkable results are found. In the following figures, fiber segregation vs. density relations are given for specimens. First, the effect of different admixtures on the segregation resistance, placeability and mechanical performance is evaluated using mix designs A_8, B_8, C_8 (6 mm fibers). After, mix designs A_2 and SCC (40 mm fibers) were evaluated together to compare CC and SCC.

Fig. 9 presents the viscosity–fiber segregation relation for mix designs A_8, B_8 and C_8. Standard deviations of the fiber contents throughout the specimen were used as a representation of segregation. As seen in Fig. 9, viscosity increases with the addition of vma and segregation decreases.

Fig. 10 presents the yield stress–density relation for mix designs A_8, B_8 and C_8. As seen in Fig. 10, the yield stress increases with addition of vma and density decreases with increasing yield stress of the cement pastes, meaning that the vma designs in this study had a high segregation resistance due to high viscosity but a low density/high pore volume due to high yield stress.

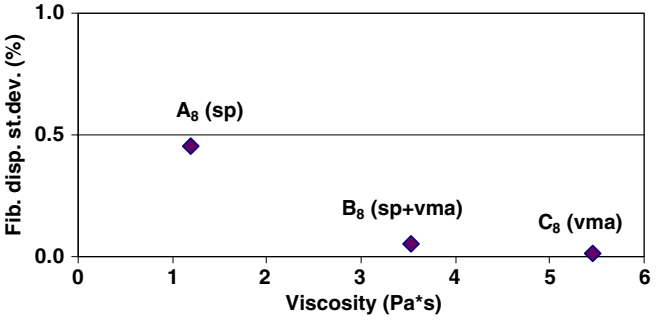

Fig. 9. Standard deviation of fiber dispersion in the specimens vs. viscosity of cement pastes.

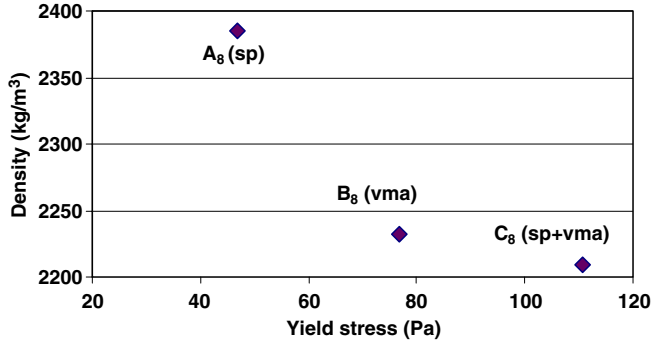

Fig. 10. Standard deviation of fiber dispersion in the specimens vs. yield stress of cement pastes.

Figs. 11 and 12 present fiber segregation vs. viscosity and density vs. yield stress relations, respectively, for conventional concrete and SCC. SCC designs are described with high viscosity and low yield stress. High viscosity ensures high segregation resistance and low yield stress provides good placeability, as a result of the high density and the superior mechanical performance. When surface quality of the specimens were compared it was seen that SCC specimens had no pores on the surface, meaning a good placeability, while the un-vibrated conventional concrete specimens had many visible pores. Vibrated conventional concrete specimens had no pores on the surface, but severe segregation inside due to vibration, as is shown in Fig. 6. This means that SCC mixes are superior to conventional concretes by means of fresh state properties, and as a result hardened state properties.

Table 7 summarizes different mix designs by means of segregation resistance, placeability, and density. It is easily seen from the table that SCC mix is superior to conventional concretes with its features.

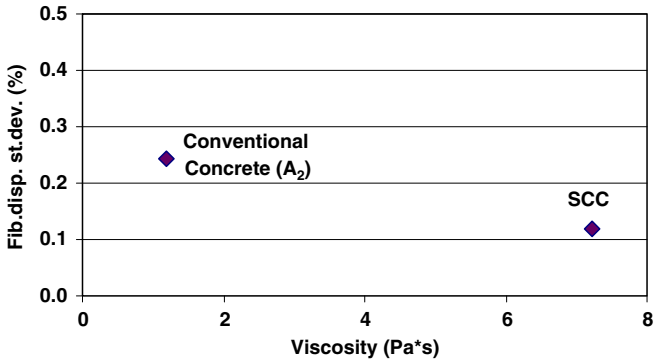

Fig. 11. Standard deviation of fiber dispersion in the specimens vs. viscosity of conventional concrete and SCC.

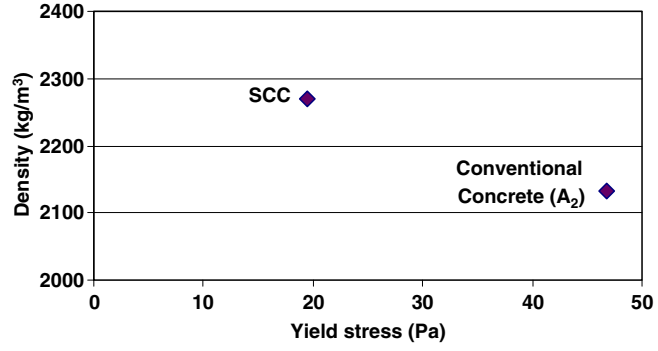

Fig. 12. Density vs. yield stress of conventional concrete and SCC.

Table 7
Comparing properties of designs

	A	B	C	SCC
Segregation	Low	High	High	Medium
Placeability	Poor	Poor	Poor	Good
Density	High	Low	Low	High

5. Conclusions

Fresh and hardened state properties of FRC specimens were connected by quantifying fiber segregation. Both conventional concretes and SCC were cast using two types of fibers. The effect of vibration time on the segregation of fibers was investigated. Rheological characteristics of the mixes were measured using a custom designed and built parallel plate rheometer. AC-IS was used to monitor fiber segregation non-destructively.

Fresh state properties were found to affect segregation of fibers and mechanical performance of FRC. Segregation increased with increasing vibration time. SCC was found to be superior to conventional concrete, with the features such as high segregation resistance, good placeability, and high mechanical performance. Vma designs also had high segregation resistance but poor placeability/low mechanical performance. These results showed that fresh state properties strongly affect fiber dispersion and mechanical performance of FRCs. This study also showed that fiber dispersion and fresh state properties can be successfully measured using the AC-IS and self-designed parallel-plate rheometer, respectively.

Acknowledgements

The authors gratefully acknowledge the financial support of Lafarge and WR-Grace. The first author also would like to acknowledge the financial support of TUBITAK (The Scientific and Technical Research Council of Turkey), Northwestern University, ITU (Istanbul Technical University) and Tincel Cultural Foundation. The authors are grateful to Dr. Katherine G. Kuder and Dr. Leta Y. Woo for helpful discussions.

Appendix. The effect of aggregate size – correction of results

Fig. A.1 can be used to explain the insulating effects of coarse aggregates. As was mentioned in the paper, the maximum aggregate size is 8 mm, while steel fibers are only 6 mm long, meaning that some of the aggregates are large enough to block conductive fibers and, therefore, may result in a decrease in the overall conductivity.

In Fig. A.1, impedance curves of mix design A_8 for concrete and cement paste are given. In Fig. A.1, R_c represents concrete resistance under high frequencies of AC, R_m shows concrete resistance under low-frequencies of AC and R_p stands for cement paste resistance. R_c and R_m were obtained from AC-IS experiments on concrete specimens and R_p was obtained from AC-IS measurements on cement paste (cement paste specimens of each concrete mix design were cast and AC-IS tests were performed on the specimens to obtain R_p). As seen in Fig. A.1, resistance of the

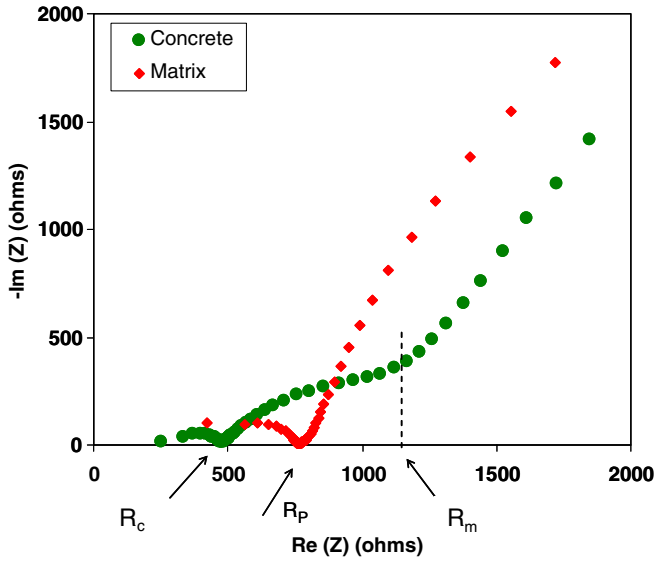

Fig. A.1. Sample Nyquist plots for concrete and cement paste of mix design A_8.

concrete matrix is higher compared to the resistance of cement paste of the same mix due to the insulating effects of the coarse aggregates. Mathematical expressions were used to exclude the insulating effect of the aggregates and to obtain corrected matrix-normalized conductivity values.

$$\frac{R_m}{R_c} = \frac{\sigma}{\sigma_m} = 1 + [\sigma]_{\infty,f}\varphi \quad (A.1)$$

$$\frac{R_p}{R_m} = \frac{\sigma_m}{\sigma_p} = 1 + [\sigma]_{0,A}\varphi_A + [\sigma]_{0,f}\varphi_f \quad (A.2)$$

$$\frac{R_p}{R_c} = \frac{\sigma}{\sigma_p} = 1 + [\sigma]_{0,A}\varphi_A + [\sigma]_{\infty,f}\varphi_f \quad (A.3)$$

In these equations

σ_m conductivity of concrete matrix, 1/Ω
σ conductivity of composite, 1/Ω
σ_p conductivity of cement paste, 1/Ω
$[\sigma]_\Delta$ intrinsic conductivity of fibers, (–)
$[\sigma]_{0,f}$ intrinsic conductivity of fibers (under low AC frequencies – insulating case)
$[\sigma]_{\infty,f}$ intrinsic conductivity of fibers (under high AC frequencies – conducting case)
$[\sigma]_{0,A}$ intrinsic conductivity of aggregates
φ_A aggregate content, %
φ_f fiber content, %

$$\frac{\sigma}{\sigma_m} = \left(\frac{R_p}{R_c} = \frac{\sigma}{\sigma_p}\right) - \left(\frac{R_p}{R_m} = \frac{\sigma_m}{\sigma_p}\right) \approx [\sigma]_{\infty,f}\varphi_f \quad (A.4)$$

Eq. (A.1) gives the general relationship between the matrix-normalized conductivity and the intrinsic conductivity when perfectly conductive fibers are used in a moderately conductive cement paste matrix. When aggregates are present in the composite material, the matrix conductivity decreases due to the insulating property of the aggregates. This results in an increase of the calculated σ/σ_m value. Eqs. (A.2) and (A.3) are used to exclude the insulating effect of the aggregates and to obtain paste matrix-normalized conductivity values. In Eq. (A.2), the term $[\sigma]_{0,f}\varphi_f$ approaches 0 due to the fact that fibers are insulating under low frequencies of AC. The term $[\sigma]_{0,A}\varphi_A$ in both equations is for insulating effect of aggregates and the term $[\sigma]_{\infty,f}\varphi_f$ in Eq. (A.3) is for the case that the fibers are conducting (high AC frequencies). Eq. (A.3) is subtracted from Eq. (A.2) to obtain the term $[\sigma]_{\infty,f.}\varphi_f$.

Observed matrix-normalized conductivity values were corrected using Eq. (A.4) for all measurements and corrected values were used for evaluations. Table 5 shows observed and corrected matrix-normalized conductivity values together with theoretical (calculated) values for the mix design A_8. It should be noted that, this correction was not needed for the mixes with 40 mm fibers due to the small size of aggregates compare to the length of the fibers.

References

[1] Banfill PFG, Beaupre D, Chapdelaine F, de Larrard F, Domone P, Nachbaur L, et al. Comparison of concrete rheometers: international tests at LCPC (Nantes, France) in October, 2000. Report NISTIR 6819, 2001.
[2] Atzeni C, Massidda L, Sanna U. Comparison between rheological models for portland cement pastes. Cem Concr Res 1985;15(3):511–9.
[3] Struble LJ, Puri U, Ji X. Concrete rheometer. Adv Cem Res 2001;13(2):53–63.
[4] Kuder K, Ozyurt N, Mu B, Shah SP. The rheology of fiber reinforced cement paste evaluated by a parallel plate rheometer. Advances in concrete through science and engineering, An international symposium during the RILEM spring meeting. Evanston (IL): Northwestern University; 2004 [on CD-Rom].
[5] Shah SP. Do fibers increase the tensile strength of cement-based matrixes? ACI Mater J 1991;88(6):595–602.
[6] Balaguru PN, Shah SP. Fiber-reinforced cement composites. New York: McGraw-Hill; 1992.
[7] Nawy EG. Fundamentals of high-performance concrete. New York: John Wiley & Sons; 2001.
[8] Banthia N, Yan C, Sakai K. Impact resistance of fiber reinforced concrete at subnormal temperatures. Cem Concr Compos 1998; 20:393–404.
[9] Shah SP, Sarigaphuti M, Karaguler ME. Comparison of shrinkage cracking performance of different types of fibers and wiremesh. In: Daniel JI, Shah SP, editors. Fiber reinforced concrete developments and innovations. Michigan: American Concrete Institute; 1994. p. 1–18.
[10] Naaman AE. Engineered steel fibers with optimal properties for reinforcement of cement composites. J Adv Concr Technol 2003;1(3):241–52.
[11] Li VC. Engineered cementitious composites. In: Banthia N et al., editors. Proceedings of ConMat'05 and mindness symposium. Canada: Vancouver; 2005 [in CD Rom].
[12] Li VC, Kanda T. Engineered cementitious composites for structural applications. J Mater Civ Eng 1998;10(2):66–9.
[13] Bentur A. Fiber-reinforced cementitious materials. In: Skalny JP, editor. Material science of concrete. The American Ceramic Society; 1989. p. 223–85.
[14] Mobasher B, Stang H, Shah SP. Microcracking in fiber-reinforced concrete. Cem Concr Res 1990;20:665–76.
[15] Ozyurt N, Woo LY, Mu B, Shah SP, Mason TO. Detection of fiber dispersion in fresh and hardened cement composites. Advances in

concrete through science and engineering. An international symposium during the RILEM spring meeting. Evanston (IL): Northwestern University [on CD-Rom].
[16] Woo LY, Wansom S, Ozyurt N, Mu B, Shah SP, Mason TO. Characterizing fiber dispersion in cement composites using AC-impedance spectroscopy. Cem Concr Compos 2005;27(6):627–36.
[17] Ozyurt N, Woo LY, Mason TO, Shah SP. Monitoring fiber dispersion in FRCs: comparison of AC-impedance spectroscopy and image analysis. ACI Mater J 2006;103(5):340–7.
[18] Ozyurt N, Correlating fiber dispersion, rheology and mechanical performance for fiber-reinforced cement-based materials. PhD thesis. Istanbul Technical University, Istanbul, 2006.
[19] Dotelli G, Mari CM. The evolution of cement paste hydration process by impedance spectroscopy. Mater Sci Eng A 2001;303:54–9.
[20] Christensen BJ, Coverdale RT, Olson RA, Ford SJ, Garboczi EJ, Jennings HM, et al. Impedance spectroscopy of hydrating cement-based materials: measurement, interpretation, and application. J Am Ceram Soc 1994;77(11):2789–804.
[21] Park G, Cudney HH, Inman DJ. Impedance-based health monitoring of civil structural components. J Infrastruc Syst 2000;6(4):153–60.
[22] Gu P, Zhongzi X, Xie P, Beaudoin JJ. An AC impedance spectroscopy study of micro-cracking in cement-based composites during compressive loading. Cem Concr Res 1993;23:675–82.
[23] Peled A, Torrents JM, Mason TO, Shah SP, Garboczi EJ. Electrical impedance spectra to monitor damage during tensile loading of cement composites. ACI Mater J 2001;98:313–22.
[24] Torrents JM, Mason TO, Garboczi EJ. Impedance spectra of fiber-reinforced cement-based composites. Cem Concr Res 2000;30:585–92.
[25] Torrents JM, Mason TO, Peled A, Shah SP, Garboczi EJ. Analysis of the impedance spectra of short conductive fiber-reinforced composites. J Mater Sci 2001;36:4003–12.
[26] Ozyurt N, Mason TO, Shah SP. Non-destructive monitoring of fiber orientation using ac-is: an industrial scale application. Cem Concr Res 2006;36(9):1653–60.
[27] Geiker ML, Brandl M, Thrane LN, Bager DH, Wallevik O. The effect of measuring procedure on the apparent rheological properties of self-compacting concrete. Cem Concr Res 2002;32:1791–5.